

Amyloid Fibrils

International Edition: DOI: 10.1002/anie.201511524
German Edition: DOI: 10.1002/ange.201511524

Polymorphism of Amyloid Fibrils In Vivo

*Karthikeyan Annamalai, Karl-Heinz Gührs, Rolf Koehler, Matthias Schmidt, Henri Michel, Cornelia Loos, Patricia M. Gaffney, Christina J. Sigurdson, Ute Hegenbart, Stefan Schönland, and Marcus Fändrich**

Abstract: Polymorphism is a wide-spread feature of amyloid-like fibrils formed *in vitro*, but it has so far remained unclear whether the fibrils formed within a patient are also affected by this phenomenon. In this study we show that the amyloid fibrils within a diseased individual can vary considerably in their three-dimensional architecture. We demonstrate this heterogeneity with amyloid fibrils deposited within different organs, formed from sequentially non-homologous polypeptide chains and affecting human or animals. Irrespective of amyloid type or source, we found *in vivo* fibrils to be polymorphic. These data imply that the chemical principles of fibril assembly that lead to such polymorphism are fundamentally conserved *in vivo* and *in vitro*.

Amyloid fibrils are linear self-assembly states of polypeptide chains.^[1] They exhibit a specific intermolecular β -sheet structure termed cross- β ,^[2,3] and occur abnormally inside the body of humans or in animals in the course of debilitating diseases, such as Alzheimer's, Parkinson's, or the various forms of systemic amyloidosis.^[1] While the precursor proteins of these pathogenic fibrils can usually be demonstrated to form fibrils inside the test tube, a fundamental but as of yet unresolved question is as to whether or not *in vitro* formed fibrils match in their structural properties with the fibrils produced inside the patient or diseased animal. This uncertainty is reflected by a recommendation of the Nomenclature Committee of the International Society of Amyloidosis, according to which *in vitro* formed fibrils shall be generally

termed "amyloid-like" to distinguish them from bona fide amyloid fibrils formed *in vivo*.^[4]

A key characteristic of fibrils formed inside a test tube is their polymorphic structure. That is, a fibrillation reaction normally gives rise to a more or less diverse spectrum of fibril morphologies.^[5,6] Changing the conditions of fibril formation affects this spectrum, makes it broader or narrower, or induces fibril ensembles consisting of different fibril states at the microscopic level. Such intra-sample polymorphism can be invisible to spectroscopic techniques, such as NMR, if the protomers possess almost identical conformations in the different polymorphs and requires single particle techniques to be resolved. While polymorphism *in vitro* has been extensively characterized,^[6-8] it is unclear whether the fibrils within a patient are also polymorphic. A recent publication suggested the A β fibrils within a given Alzheimer's disease patient to be homogeneous, but to differ from one patient to another.^[9] Such a scenario was suggested to be relevant, for example, in the context of personalized medicine approaches.^[10] However, the conclusions presented in that study were not obtained by investigating patient fibrils themselves but from a NMR-spectroscopic analysis of isotopically labeled fibrils grown in the presence of brain homogenates and fibril seeds *in vitro*.

Herein, we have extracted fibrils from different amyloidotic tissues and analyzed their structural morphology directly at the single particle level with transmission electron microscopy (TEM). The used procedures to purify fibrils is based on the original water extraction method that depends on the solubility of fibrils in water.^[11] We here demonstrate the performance of our extraction procedure with fibrils purified from the heart of a 51 year old woman, suffering from light chain (AL) amyloidosis. Fibrils are clearly visible by TEM under negative staining conditions (Figure 1 A). Denaturing polyacrylamide gel electrophoresis shows the relatively high purity of the fibril protein and the presence of one major protein species at approximately 12 kDa (Figure 1 B). Using Edman degradation and mass spectrometry we determined the amino acid sequence of the AL protein constructing the fibril (Supporting Information, Figure S1 A). We find that it corresponds to an N-terminal fragment of a λ 1 light chain that was obtained by cDNA sequencing of the malignant λ restricted plasma cell clone that caused AL amyloidosis in this patient (Supporting Information, Figure S1 A). Mass spectrometry determines the mass of the AL protein at 12168 ± 4 Da (Supporting Information, Figure S1 B), which corresponds well to the theoretic mass expected from the sequence (12167 Da).

[*] K. Annamalai, Dr. M. Schmidt, H. Michel, C. Loos, Prof. Dr. M. Fändrich
Institute of Protein Biochemistry, Ulm University
Helmholtzstrasse 8/1, 89081 Ulm (Germany)
E-mail: marcus.faendrich@uni-ulm.de

Dr. K.-H. Gührs
CF Proteomics
Leibniz Institute on Aging—Fritz Lipmann Institute (FLI)
Beutenbergstraße 11, 07745 Jena (Germany)

Dr. R. Koehler
Institute of Human Genetics
Im Neuenheimer Feld 366, 69120 Heidelberg (Germany)

Dr. P. M. Gaffney, Prof. Dr. C. J. Sigurdson
Department of Pathology, University of California, San Diego
9500 Gilman Drive, MC 0162, La Jolla, CA 92093-0612 (USA)

Priv.-Doz. Dr. U. Hegenbart, Priv.-Doz. Dr. S. Schönland
Amyloidosis Center, Department of Internal Medicine V
Im Neuenheimer Feld 410, 69120 Heidelberg (Germany)

Supporting information for this article can be found under:
<http://dx.doi.org/10.1002/anie.201511524>.

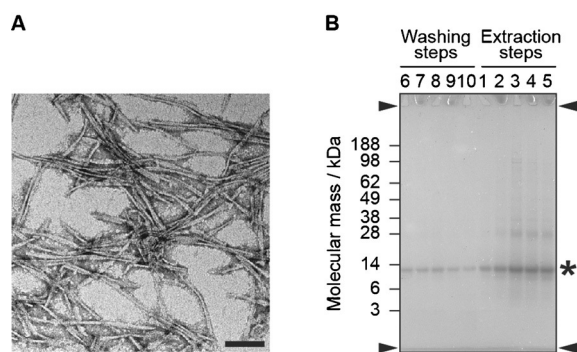


Figure 1. A) Negative-stain TEM image of the fibrils extracted from the AL case 1 heart tissue samples. Scale bar: 100 nm. B) Coomassie-stained denaturing polyacrylamide gel run under reducing conditions showing the last five washing steps with Tris-EDTA and the first five extraction steps in water. The asterisk indicates the AL protein. Arrow heads show gel border.

The extracted fibrils show key features of amyloid and stain with classical amyloid binding dyes, such as Congo red and Thioflavin T (Supporting Information, Figure S2A,B). They also give rise to Congo red green birefringence when viewed in a polarizing microscope. Attenuated total reflectance Fourier transform infrared spectroscopy shows high β -sheet content (Supporting Information, Figure S2C) evident from the amide I maximum at 1636 cm^{-1} .

Analysis of the fibril morphology with TEM and quantitative assessment of the fibrillar morphology by measurement of the helical pitch, the width and the apparent width of the fibril at its crossovers (Figure 2A) reveals the fibrils from this AL patient to fall in at least two different groups, termed here morphologies I and II (Figure 2B,C). Morphology I is mark-

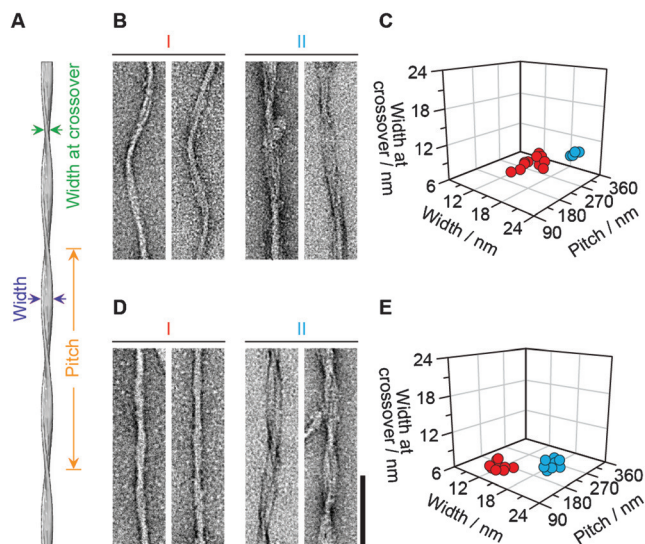


Figure 2. A) Representation of the parameters fibril width, pitch, and width at the crossover based on the electron microscopy data bank entry EMD-3132.^[12] Negative-stain TEM images of AL amyloid fibrils (case 1, B) and plot of the structural parameters (C). Negative stain TEM images of AL amyloid fibrils (case 2, D) and plot of the structural parameters (E). Scale bar: 100 nm.

edly thinner (average width $14 \pm 1.4\text{ nm}$) than morphology II (average width $19 \pm 0.8\text{ nm}$) and shows a less well-pronounced crossover structure (Figure 2B). We made very similar observations with a second case of human cardiac AL amyloidosis where fibrils were extracted from an explanted heart of a 56 year old woman (Supporting Information, Figure S3A). These fibrils comprise a different light chain fragment as AL protein (Supporting Information, Figure 3B) compared to case 1 but show typical amyloid characteristics upon dye binding or infrared as well (Supporting Information, Figure S4). Furthermore, we found at least two well-resolved fibril morphologies that varied by their average width ($11.6 \pm 0.6\text{ nm}$ vs. $20.6 \pm 1.3\text{ nm}$) and pitch ($163 \pm 7\text{ nm}$ vs. $212 \pm 23\text{ nm}$, Figure 2D,E); that is, morphology I is thinner, while morphology II presents a more clearly resolved cross-over structure.

Having established the polymorphism of fibrils in both cases of AL amyloidosis we turned to human mutant transthyretin (mt-ATTR) amyloidosis. We investigated the morphology of the fibril that we have extracted from an explanted heart of a 64 year old man, carrying the Val40Ile mutation. Again there is more than one well-resolved fibril morphology, two of which are represented here. Morphology I is thinner and lacks a clearly visible crossover structure, while morphology II shows a clearly resolved periodicity along the fibril main axis (Figure 3A).

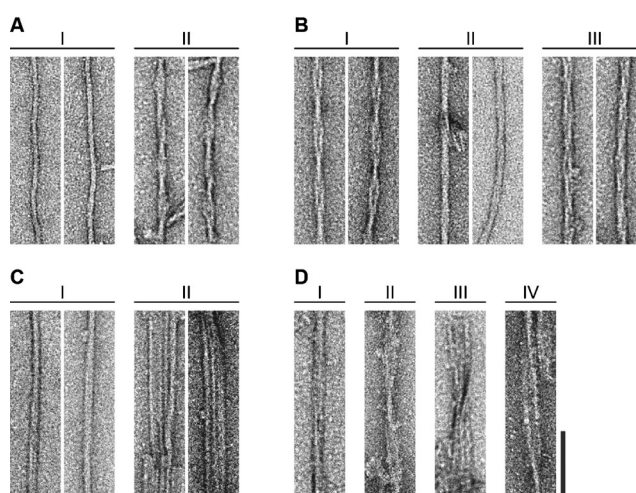


Figure 3. Negative-stain mt-ATTR amyloid fibrils from human heart (A) and of AA amyloid fibrils from mouse spleen (B), fox spleen (C), and goat uterus (D). Scale bar: 100 nm.

Polymorphism is not only associated with the fibrils formed in humans, it is also seen with fibrils deposited in animals. This observation is demonstrated here with fibrils extracted from the spleens of AA amyloidotic mice (*Mus musculus*, Figure 3B),^[13] or island foxes (*Urocyon littoralis*, Figure 3C),^[14] as well as from the uterus of an AA amyloidotic goat (*Capra aegagrus hircus*, Figure 3D).^[15] These fibrils are derived from SAA1 (mouse),^[13] SAA3 protein (goat),^[15] and from homologue of SAA1 or SAA2 in fox.^[14] In all cases we find the co-existence of multiple fibril morphologies as

defined by TEM (Figure 3B–D). Importantly, samples usually contained fibril morphologies beyond the examples selected here for presentation and we could extract and analyze only a small fraction of all the fibrils present in a diseased animal or patient.

We conclude that each patient and each diseased animal investigated here comprises multiple fibril morphologies and that polymorphism is a wide-spread, if not a conserved, feature of amyloid fibrils formed *in vivo*. It affects fibrils derived from non-homologous proteins that are deposited in different organs and that cause disease in humans or animals. Our data relate to previous observations reporting variations in the binding of different dyes to histological sections that could potentially arise from fibril polymorphism.^[16,17] By contrast, there was no evidence that the extraction procedure would destroy the morphology of preformed fibrils added to the tissue prior to carrying out an extraction (Supporting Information, Figure S5).

Polymorphism arises if fibrils differ in the number of their constituting protofilaments, if the protofilaments possess different relative orientations, or if they exhibit a different internal structure.^[18] While differences in the relative arrangement of the protofilaments imply altered interaction surfaces between the protofilaments,^[5] differences in their substructure testify to different conformations and/or arrangements of the polypeptide chains within a protofilament.^[19] Polymorphism arises from the formation of differently structured fibril nuclei and their extension into different fibril morphologies. This notion is supported by previous evidence for the inherently stochastic nature of fibril nucleation^[20] and molecular dynamics simulations demonstrating that the ensemble of formed fibril morphologies can be controlled by kinetic factors.^[21]

The process of fibril formation is obviously dependent on the environmental conditions because changing the temperature or solution composition alters the set of favorable interactions between the fibril forming polypeptide chains. However, we have only a limited understanding of how particular solution conditions lead to certain fibril ensembles. A study of A β fibril morphologies suggested that increasing the concentration of kosmotropic salts favors the formation of fibril morphologies that are associated with a better burial of surface exposed hydrophobic groups.^[22] Inside a cell, factors such as macromolecular crowding, molecular chaperones or lipid bilayers may additionally influence the development of certain fibril morphologies.

Another factor contributing to the formation of different fibril morphologies is associated with the templated growth of these fibrils or seeding. Such mechanisms are likely relevant *in vivo*. One example hereof is the glycosaminoglycan induced growth of fibrils.^[23] The interactions with the regular pattern of the polysaccharide can probably induce the particular fibril architectures or ensembles of fibril architectures. This possibility is also highlighted in the case of prion strains where different prion structures induce their own replication and specific disease phenotype.^[2] Whether these effects suffice to induce the formation of only one fibril morphology in a given patient has so far remained unclear.

Our present observation of structural polymorphism in a diverse set of amyloid fibrils formed *in vivo* demonstrates that factors like these are evidently not strong enough to prevent the formation of polymorphic fibril structures in the examined cases. Hence, self-assembly of polypeptide chains *in vivo* follows similar chemical principles of fibril assembly and variations in the fibril nucleation process as fibril formation reactions occurring within a test tube.

Experimental Section

Fibril extraction: Fibrils were extracted from all the amyloid-laden tissue using a method that was based upon a water-extraction procedure.^[11] In brief, 250 mg of tissue material were diced with scalpel and washed 5 times with 0.5 mL Tris calcium buffer (20 mM Tris, 138 mM NaCl, 2 mM CaCl₂, 0.1% NaN₃, pH 8.0). Each washing step consisted of gentle vortexing and centrifugation at 3,100 g for 1 minute at 4°C. The supernatant was discarded and the pellet was resuspended in 1 mL of freshly prepared 5 mg mL⁻¹ *Clostridium histolyticum* collagenase (Sigma) in Tris calcium buffer. After incubation overnight at 37°C in a horizontal orbital shaker at 750 rpm the tissue material was centrifuged at 3,100 g for 30 min at 4°C and the supernatant was removed. The retained pellet was resuspended in 0.5 mL Tris ethylenediaminetetraacetic acid (EDTA) buffer (20 mM Tris, 140 mM NaCl, 10 mM EDTA, 0.1% NaN₃, pH 8.0) and homogenized with a Kontes pellet pestle using 5 cycles consisting of one second on and one second off. The homogenate was centrifuged for 5 min at 3,100 g at 4°C and the supernatant was removed carefully. This step was repeated nine more times. After the tenth homogenization step with Tris-EDTA buffer, the remaining tissue pellet was homogenized with a Kontes pellet pestle in 0.5 mL of ice cold water. The homogenate was centrifuged for 5 minutes at 3,100 g at 4°C and the supernatant was removed and stored as water extract 1. This step was repeated nine more times.

Negative-stain TEM specimens were prepared by placing 5 μ L of the sample solution on to a formvar and carbon coated 200 mesh copper grid (Plano). After incubation for 1 minute at room temperature, the excess solution was carefully soaked away with filter paper. Subsequently, the grid was washed three times with water and stained three times with 2% (w/v) uranyl acetate solution. Grids were examined in a JEM-1400 TEM (JEOL) that was operated at 120 kV. ImageJ software was used to measure the fibril pitch, width and width at crossover from the electron micrographs. The collected data points were plotted by using Origin software.

Acknowledgements

We want to heartily thank the reported patients and their families for supporting our research activities with the donation of their explanted hearts. This work is supported by the Bundesministerium für Forschung und Bildung (BMBF, GERAMY network on systemic AL amyloidosis in Germany, FKZ 01GM110), and a grant from the Deutsche Forschungsgemeinschaft to M.F. (FA 456/15-1). We thank the Departments of Cardiology and Cardio-Surgery, University Hospital Heidelberg, for their support.

Keywords: Alzheimer's disease · Parkinson's disease · prions · protein folding · systemic amyloidosis

How to cite: *Angew. Chem. Int. Ed.* **2016**, *55*, 4822–4825
Angew. Chem. **2016**, *128*, 4903–4906

- [1] F. Chiti, C. M. Dobson, *Annu. Rev. Biochem.* **2006**, *75*, 333–366.
- [2] D. Eisenberg, M. Jucker, *Cell* **2012**, *148*, 1188–1203.
- [3] M. Sunde, L. C. Serpell, M. Bartlam, P. E. Fraser, M. B. Pepys, C. C. Blake, *J. Mol. Biol.* **1997**, *273*, 729–739.
- [4] J. D. Sipe, M. D. Benson, J. N. Buxbaum, S. Ikeda, G. Merlini, M. J. Saraiva, P. Westermark, *Amyloid* **2014**, *21*, 221–224.
- [5] J. Meinhardt, C. Sachse, P. Hortschansky, N. Grigorieff, M. Fändrich, *J. Mol. Biol.* **2009**, *386*, 869–877.
- [6] C. S. Goldsbury, G. J. Cooper, K. N. Goldie, S. A. Müller, E. L. Saafi, W. T. Gruijters, M. P. Misur, A. Engel, U. Aebi, J. Kistler, *J. Struct. Biol.* **1997**, *119*, 17–27.
- [7] R. Kodali, A. D. Williams, S. Chemuru, R. Wetzel, *J. Mol. Biol.* **2010**, *401*, 503–517.
- [8] J. L. Jiménez, E. J. Nettleton, M. Bouchard, C. V. Robinson, C. M. Dobson, H. R. Saibil, *Proc. Natl. Acad. Sci. USA* **2002**, *99*, 9196–9201.
- [9] J. X. Lu, W. Qiang, W. M. Yau, C. D. Schwieters, S. C. Meredith, R. Tycko, *Cell* **2013**, *154*, 1257–1268.
- [10] A. Aguzzi, A. D. Gitler, *Cell* **2013**, *154*, 1182–1184.
- [11] M. Pras, M. Schubert, D. Zucker-Franklin, A. Rimon, E. C. Franklin, *J. Clin. Invest.* **1968**, *47*, 924–933.
- [12] M. Schmidt, A. Rohou, K. Lasker, J. K. Yadav, C. Schiene-Fischer, M. Fändrich, N. Grigorieff, *Proc. Natl. Acad. Sci. USA* **2015**, *112*, 11858–11863.
- [13] K. Lundmark, G. T. Westermark, S. Nyström, C. L. Murphy, A. Solomon, P. Westermark, *Proc. Natl. Acad. Sci. USA* **2002**, *99*, 6979–6984.
- [14] P. M. Gaffney, D. M. Imai, D. L. Clifford, M. Ghassemian, R. Sasik, A. N. Chang, T. D. O'Brien, J. Coppinger, M. Trejo, E. Masliah, L. Munson, C. Sigurdson, *PLoS One* **2014**, *9*, e113765.
- [15] P. M. Gaffney, B. Barr, J. D. Rowe, C. Bett, I. Drygiannakis, F. Giannitti, M. Trejo, M. Ghassemian, P. Martin, E. Masliah, C. J. Sigurdson, *FASEB J.* **2015**, *29*, 911–919.
- [16] G. Heilbronner, Y. S. Eisele, F. Langer, S. A. Kaeser, R. Novotny, A. Nagarathinam, A. Aslund, P. Hammarström, K. P. Nilsson, M. Jucker, *EMBO Rep.* **2013**, *14*, 1017–1022.
- [17] J. Bergström, A. Gustavsson, U. Hellman, K. Sletten, C. L. Murphy, D. T. Weiss, A. Solomon, B. O. Olofsson, P. Westermark, *J. Pathol.* **2005**, *206*, 224–232.
- [18] M. Fändrich, J. Meinhardt, N. Grigorieff, *Prion* **2009**, *3*, 89–93.
- [19] J. J. Wiltzius, M. Landau, R. Nelson, M. R. Sawaya, M. I. Apostol, L. Goldschmidt, A. B. Soriaga, D. Cascio, K. Rajashankar, D. Eisenberg, *Nat. Struct. Mol. Biol.* **2009**, *16*, 973–978.
- [20] T. Christopeit, P. Hortschansky, V. Schroeckh, K. Gührs, G. Zandomeneghi, M. Fändrich, *Protein Sci.* **2005**, *14*, 2125–2131.
- [21] R. Pellarin, P. Schuetz, E. Guarnera, A. Caflisch, *J. Am. Chem. Soc.* **2010**, *132*, 14960–14970.
- [22] K. Klement, K. Wieligmann, J. Meinhardt, P. Hortschansky, W. Richter, M. Fändrich, *J. Mol. Biol.* **2007**, *373*, 1321–1333.
- [23] J. McLaurin, T. Franklin, X. Zhang, J. Deng, P. E. Fraser, *Eur. J. Biochem.* **1999**, *266*, 1101–1110.

Received: December 11, 2015

Published online: March 8, 2016